Trends and strain in the structures of two-dimensional rare-earth silicides studied using medium-energy ion scattering

C. Bonet,[1] I. M. Scott,[1] D. J. Spence,[1] T. J. Wood,[1] T. C. Q. Noakes,[2] P. Bailey,[2] and S. P. Tear[1,*]
[1]*Department of Physics, University of York, Heslington, York, YO10 5DD, United Kingdom*
[2]*CCLRC Daresbury Laboratory, Daresbury, Warrington, WA4 4AD, United Kingdom*
(Received 7 July 2005; published 6 October 2005)

The surface structures of the two-dimensional (2D) rare-earth (RE) silicides formed by Gd and Tm on Si(111) have been determined using medium-energy ion scattering (MEIS). These data have been taken together with those from earlier MEIS studies of the 2D silicides formed by Dy, Ho, Er, and Y to investigate the existence of trends in the structural parameters of this class of surfaces. It was found that the Si-RE bond length associated with the surface bilayer in the 2D silicides followed the same trend as the bond length in the bulk silicide compounds which is simply related to the size of the RE atom. In contrast, changes in the Si-RE layer spacing in the 2D silicides were found to be too large to be accounted for by a size effect alone. It was found that the strain that results from the expansion or compression of the overlayer to fit the Si(111) surface is compensated by changes in the Si-RE layer spacing. Finally, there is a systematic variation in the rumple of the surface bilayer in the 2D RE silicides which appears to increase with the magnitude of the lattice mismatch suggesting that strain in the overlayer results in a weakening of the Si-Si bond in the surface bilayer.

DOI: 10.1103/PhysRevB.72.165407 PACS number(s): 68.55.−a, 68.65.−k, 68.35.Ct, 68.49.Sf

I. INTRODUCTION

In recent years a considerable amount of scientific activity has been associated with studies of the metal-semiconductor interface. Such studies are often motivated because of the technological importance of this work that arises as a result of the relevance of these interfaces to the electronic device industry. The nature of the metal-semiconductor interface is however also interesting from a fundamental perspective. A detailed knowledge of the structures formed at these interfaces is valuable in terms of developing an understanding of both the origin of defects (which may have deleterious effects on ultimate device properties) and the influence that the geometrical arrangement may have on the electronic structure of the interface.

In particular, the rare-earth (RE) silicides grown on Si(111) have attracted considerable interest[1] in part due to the identification of unusually low Schottky barrier heights (~0.3–0.4 eV) on *n*-type Si.[2,3] The bulk silicides formed by the trivalent RE metals have a defect-AlB_2 structure in which hexagonal layers of RE atoms are located between graphitelike layers of Si atoms which contain an ordered array of vacancies. Furthermore, these bulk silicides have a generally good lattice match to the Si(111) surface with degrees of mismatch ranging from ~1% to ~−3% which is encouraging from the point of view of achieving epitaxial growth.[4]

The discovery of the two-dimensional (2D) phases of the RE silicides on Si(111) (Refs. 5 and 6) which are formed from a single monolayer of a trivalent RE metal provided the opportunity to study the very first stages of silicide-silicon interface formation and to date a number of techniques (including AED,[6,7] SEXAFS,[7] SXRD,[8] quantitative LEED,[9–11] and MEIS[8,12–14]) have been employed to study structural aspects in these systems. In the 2D RE silicide, a single monolayer of RE atoms are located above T4 sites of a bulklike Si(111) surface. Above these RE atoms lies a single Si bilayer with its buckling direction reversed (referred to as type B orientation) with respect to that of bulk silicon. A diagram of this structure can be found in Fig. 1.

The existence of a series of chemically similar rare-earth elements from Gd to Tm which all form 2D silicides provides the possibility of studying trends in the structural parameters of these surfaces. In terms of determining the surface structure above the RE layer, the technique of medium-energy ion scattering (MEIS) is particularly well suited to the task as a result of the large mass difference between RE and Si atoms. This permits the separate extraction and analysis of the angle-dependent RE scattering yield, which contains only information relating to the positions of atoms Si1 and Si2 (notation as indicated in Fig. 1) relative to the RE atom. Thus by exploiting the ability of MEIS to focus on particular aspects of the surface structure, the number of parameters influencing any given data set is reduced. This permits one to have confidence in the resulting structural data since the mutual interaction of fitting parameters is reduced to an absolute minimum and effects due to the influence of any substrate relaxation are completely eliminated. A further advantage of the technique of MEIS in the present class of systems is the way in which structural parameters and nonstructural parameters (such as vibrational amplitudes) have characteristically different effects on the experimental data, effects which most importantly are separable.

The influence of strain at surfaces and at interfaces during epitaxial growth is an important topic in both fundamental and applied research and has recently attracted much interest. For example, Intel has already utilized strained silicon in a production 90 nm device process to improve mobility. Furthermore, anisotropic strain resulting from lattice mismatch has recently been proposed as the driving force behind the formation of "nanowires" during the initial stages of RE silicide growth on Si(001).[15,16] Characterization of the effect of strain on the electronic properties at a silicide-silicon inter-

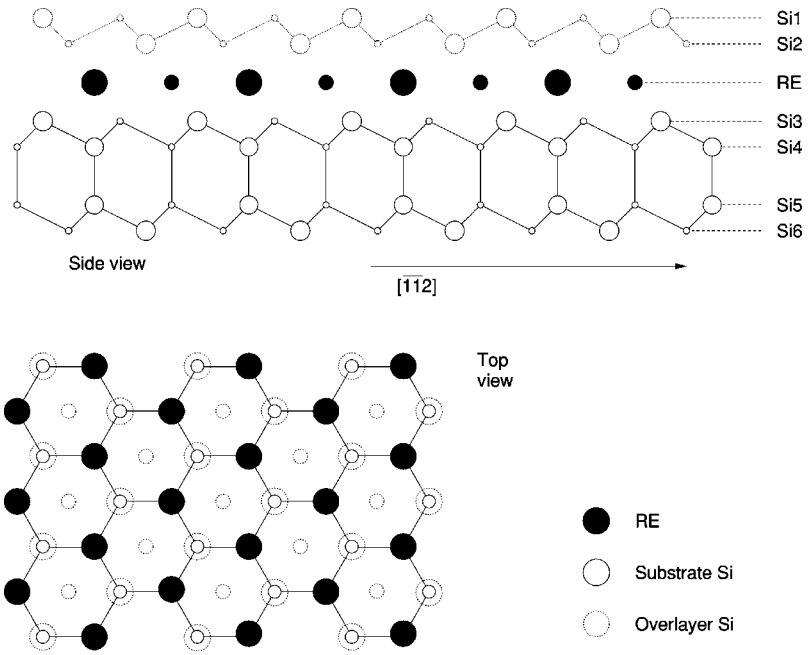

FIG. 1. Diagram showing the surface structure of the 2D rare-earth silicides.

face could have potential technological value (with the possibility of exploiting these effects through control of strain). An important key to interpreting such behavior would be a precise knowledge of the associated changes in atomic structure and it is this aspect that the present study sets out to address. The variation in the lattice matches of the bulk RE silicides with Si(111) has permitted the examination of the effect of strain on the very initial stages of interface formation through the study of the structures of the 2D RE silicides.

The results presented in this paper relate to MEIS studies of the 2D silicides formed by the rare-earth elements Gd, Dy, Ho, Er, Tm, and Y (although Y is not formally a member of the lanthanides, it is considered to be a rare-earth element due to its chemical similarity). The experimental data concerning Gd and Tm have not previously been reported, whereas for Dy, Ho, Er, and Y the data have been published elsewhere.[12–14] In the case of Dy, Ho, and Er the analysis presented here differs from that previously reported[12,13] due to the identification of issues associated with the *R*-factor (used to fit the data to simulations) which are elaborated on in the following text.

The remainder of this paper is organized as follows. First, the experimental aspects are detailed, including sample preparation and the particulars of the ion scattering experiments and simulations. Then the data and its analysis are described together with a discussion of the behavior of the *R*-factor used to compare simulation and experiment and the potential influence of this upon the results. The optimized structural parameters for all the 2D RE silicides mentioned above are then given and these results are discussed in the context of trends and strain. Finally, the findings of this study are summarized.

II. EXPERIMENT

All MEIS data were obtained at the UK MEIS facility at CCLRC Daresbury Laboratory. The facility is described in detail elsewhere.[17] Samples were prepared starting with an approximately 10 mm $\times$ 10 mm section cut from a lightly doped *n*-type Si(111) wafer. These were introduced into a UHV chamber with a base pressure of $<3\times10^{-10}$ mbar and after degassing were flash-heated to $\sim$1200 °C for 1 min by *e*-beam bombardment from the reverse side. After slowly cooling to room temperature the resulting surface showed a sharp 7×7 LEED pattern characteristic of the clean, well-ordered surface. Deposition of one monolayer (ML) of RE metal onto the room temperature Si surface was carried out using home-made evaporation sources that contained the RE metal within either a W filament (in the case of Gd, Ho, Dy, and Y) or a Ta boat (for Tm), while the deposition of Er utilized a commercial K-cell evaporator. The subsequent annealing of the samples to $\sim$500 °C for $\sim$10 min resulted in the formation of the ordered 2D silicide surface, as evidenced by a sharp 1×1 LEED pattern with low background intensity. The absence of features in the LEED pattern that could be associated with other reconstructions in the RE/Si(111) system confirmed that the RE coverage was close to 1 ML (where 1 ML is defined relative to the 1×1 surface unit cell, i.e., an areal atomic density of 7.83×10^{18} m^{-2}). Typically one would estimate the precision with which the RE coverage is controlled to be $\sim$20%.

The prepared samples were transferred under UHV into the ion scattering chamber which operated with a base pressure of $<3\times10^{-10}$ mbar. MEIS data were taken using a H^+ beam with a nominal energy of 100 keV and which was collimated to result in a beam size of 1.0 mm $\times$ 0.5 mm at the sample. The total ion dose used to collect the surface data was $\sim10^{16}$ ions cm^{-2} the exact value depending on the particular scattering geometry employed. For each sample two channelling geometries were used, one in which the ion beam was incident along a $[\bar{1}00]$ direction and the other using $[1\bar{1}\bar{1}]$ incidence (except in the case of Y where the latter geometry was substituted by $[\bar{1}\bar{1}0]$ incidence). In each case the angle-dependent RE scattering yield was extracted

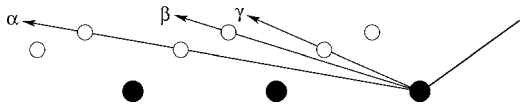

FIG. 2. The origin of the blocking dips in the RE scattering yield for the $[\bar{1}00]$ incidence geometry. The filled and open circles represent Y atoms and Si atoms in the surface bilayer, respectively.

from the raw experimental data, and the resulting blocking curve was used to determine the positions of atoms Si1 and Si2 relative to the RE atom. Simulated blocking curves for a range of models were generated by a Monte Carlo method[18,19] using the XVegas code[20] and a quantitative comparison with experiment was made using the χ^2 R-factor.[21]

III. RESULTS AND DISCUSSION

The blocking curves obtained from the 2D RE silicides can be readily interpreted in terms of the surface structure. For the $[\bar{1}00]$ incidence geometry, Fig. 2 illustrates the origin of the blocking dips in the RE scattering yield. It can be seen that the dips labelled β and γ each contain only information relating to a single surface atom (Si1 and Si2, respectively) whereas the dip α arises as a result of contributions from both Si1 and Si2.

The angle-dependent RE scattering yield for the 2D silicides formed by a variety of RE elements is plotted in Fig. 3 for scattering angles from 54° to 61° and shows dip γ which contains only information relating to the location of atom Si2. In this figure the origin of the yield axis has been offset between curves so as to vertically separate the plots and the curves have been stacked (from bottom to top) in a sequence which corresponds to an increase in the RE-Si bond length in the bulk $RESi_{1.7}$ compound. Since the lateral position of atom Si2 is constrained by the symmetry and 1×1 periodicity of the surface, variations in the position of the dip shown in Fig. 3 can directly be interpreted as changes in the z coordinate (where the z axis is taken to be parallel to the surface normal) of atom Si2. The data presented in this plot thus shows quite clearly a systematic trend in the RE-Si2 layer spacing.

A. Fitting experimental data to simulation

It was mentioned above that the χ^2 R-factor was used as a quantitative measure of the level of agreement between experimentally measured blocking curves and those obtained from simulations of model structures. Whilst the χ^2 R-factor has been successfully used in a number of MEIS studies over the years, during the course of the present work the sensitivity of the R-factor to nonstructural parameters was highlighted. In a structural study one would ideally wish to employ a R-factor which had low (or zero) sensitivity to nonstructural parameters (such as vibrational amplitudes), i.e., a R-factor which was sensitive to the positions of dips in the blocking curves. In contrast, the χ^2 R-factor is sensitive to the overall level of agreement between the data and simulation, and thus identifies as the best fit the model which results in a blocking curve that is generally the closest match

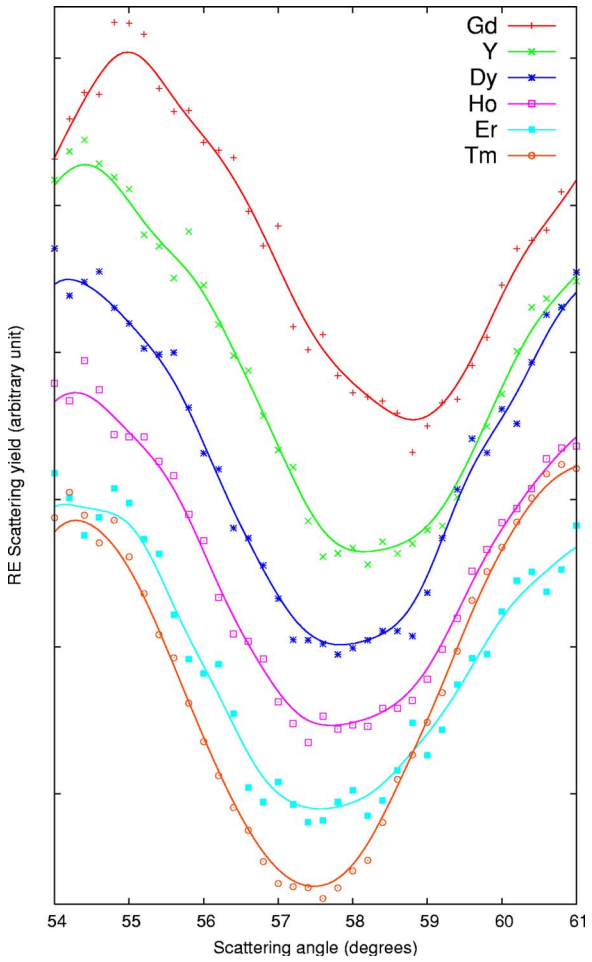

FIG. 3. (Color online) Angle-dependent RE scattering yield for the $[\bar{1}00]$ incidence geometry in the region of the dip γ for a range of 2D silicides. A curve drawn through a smoothed version of raw experimental data has been added to guide the eye. Data shown for Gd and Tm not previously reported; others from Refs. 12–14.

to the experimental data even if that model is not structurally the best model.

The sensitivity of the χ^2 R-factor to nonstructural parameters can be seen in Fig. 4(a) which shows a comparison between experiment and simulation for the model identified as optimal by the R-factor. The square of the residuals at each angle, weighted to take into account the associated statistical significance and expressed as a percentage of this quantity summed over all angles is also shown on this plot and illustrates the origin of contributions to the R-factor. It can be seen that the model selected is one in which the positions of dips β and γ in the simulation are not precisely aligned with the experimental data, indicating that atoms Si1 and Si2 have been displaced from their correct positions. The reason for this behavior is apparent in Fig. 4(b) which shows a similar plot corresponding to a simulation of the model which is structurally the best fit, as indicated by the correct angular positions of all three dips. In this case the largest contribution to the R-factor results from the disagreement in the depth of the dip α. In the fitting process this nonstructural contribution to the R-factor has been reduced by displacing

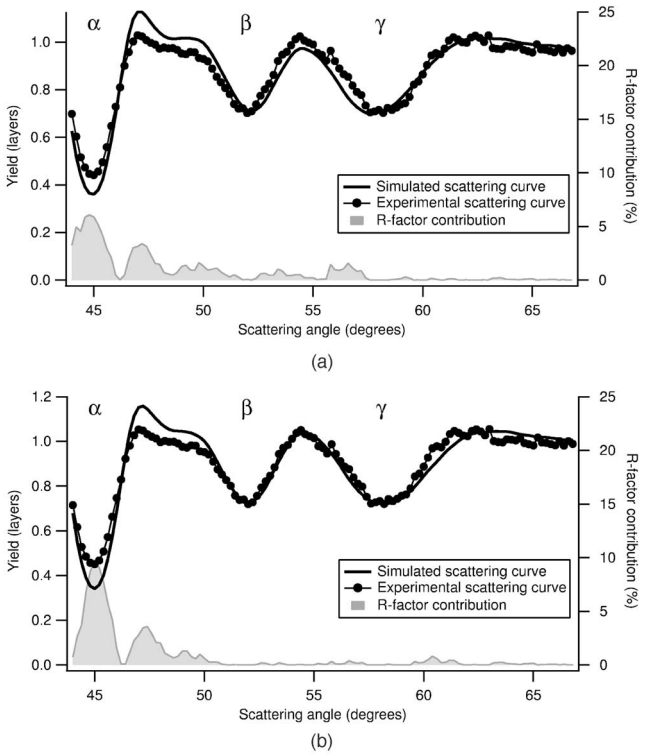

FIG. 4. Plot illustrating the origin of contributions to the χ^2 *R*-factor (weighted square of the residuals) when comparing experimental data to a simulation for (a) the optimum model selected by the *R*-factor and (b) the structurally correct model. (Experimental data corresponds to 2D yttrium silicide, Ref. 14.)

Si1 and Si2 so as to broaden and reduce the depth of dip α, resulting in the optimum fit shown in Fig. 4(a) which does not correspond to the best structural model. In the case illustrated the contribution from dip α is particularly large as a result of the discrepancy occurring at low scattering angles. As a consequence of the Rutherford scattering cross section, low scattering angle data contains a greater number of counts, is thus statistically more significant, and is weighted accordingly by the χ^2 *R*-factor. The result of this behavior is that the χ^2 *R*-factor exhibits a preference for models containing structural changes which lessen the depth of dip α, even if such changes lead to disagreement in the positions of the higher scattering angle dips β and γ.

It is clear from the above that provided both the structural and nonstructural aspects of the simulation are correct, then the χ^2 *R*-factor will select as the optimum model that which is structurally correct and therefore the use of the χ^2 *R*-factor in MEIS structural analyses is entirely appropriate. On the other hand, in the early stages of a structural search neither the structural parameters nor the nonstructural parameters are known, so the implication of this behavior of the χ^2 *R*-factor is that every plausible combination of both structural and nonstructural parameters must initially be tried. This is undesirable (as it is computationally very expensive) and one possible solution is to employ in the early stages of optimization a *R*-factor which is sensitive to the positions of the dips rather than the overall level of agreement between the experimental and simulated blocking curves.[22]

A consistent feature of the MEIS analyses of the 2D RE silicides was the finding that in each case the depth of dip α in the simulations was excessive in comparison to the experimental data when both β and γ fitted well. Since both the positions and vibrational amplitudes of atoms Si1 and Si2 can be independently fitted via dips β and γ, respectively, it was possible to eliminate (isotropic) vibrational effects as a possible cause of this discrepancy. Other causes of this effect including anisotropic vibrations, correlations in the vibrations of surface atoms, and static disorder (in various forms) have been considered. One possible source of the extra yield recorded in the experiment in the region of dip α was identified as a very slight out-of-plane misalignment of the analyzer.

Such an analyzer misalignment can take one of two forms, either a vertical displacement between the point that the incident ion beam hits the sample and the entrance slit of the analyzer or a slight rotation of the azimuthal direction along which ions are detected. The former was measured and found to be 0.25 mm and was subsequently taken account of in the simulations. It was not possible to measure any azimuthal misalignment due to the disruptive effect that this would have on the operation of the MEIS facility, however a value of 0.5° was found to bring the depth of dip α into agreement for all the 2D RE silicides[24] and this value is not unreasonable for the precision with which a large mechanical system can be aligned. While the absence of a measurement of this aspect of the instrument alignment means it is not possible to conclusively identify this as the cause of the unexpected depth of dip α, our aim in this work is to determine the structural parameters of these surfaces and these small misalignments do not have a detectable effect on the positions of the dips. It is only necessary to correct for these effects in order to ensure that the selection of the correct structural model by the χ^2 *R*-factor is not impaired by disagreements in the nonstructural aspects of the simulation.

During the course of this work it became apparent that if the MEIS structural analyses of the 2D RE silicides were to be used to investigate subtle trends in these structures, then in order to obtain structural parameters of the required accuracy it was necessary to include the corrections described above in order to ensure the correct operation of the χ^2 *R*-factor. The results which are presented below correspond to the optimum structural models as selected by the χ^2 *R*-factor after the application of these corrections to the simulations. The earlier MEIS structural results for Er,[12] Ho,[12] and Dy,[13] have been refined in light of these findings in order to ensure that all the data used in this study has been analyzed in a consistent manner.

The experimentally measured RE scattering yield from the $[\bar{1}00]$ incidence geometry is shown together with the simulation for the optimum model in Figs. 5 and 6 for the 2D silicides formed by Gd and Tm, respectively. These plots show that once nonstructural sources of discrepancies have been eliminated, the χ^2 *R*-factor is able to correctly identify the model with optimum structural parameters, as evidenced by the level of agreement in the positions of all three blocking dips in Figs. 5 and 6. The final set of structural parameters was selected by the *R*-factor as the optimal fit based on

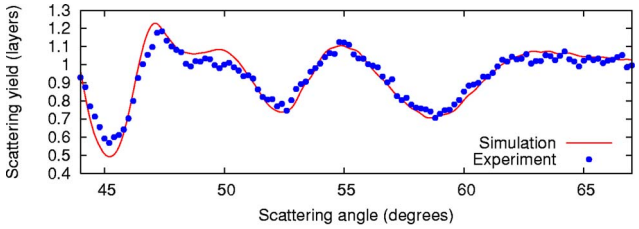

FIG. 5. (Color online) The angle-dependent RE scattering yield from Si(111)1×1-Gd for the $[\bar{1}00]$ incidence geometry shown along with the simulation for the optimum model.

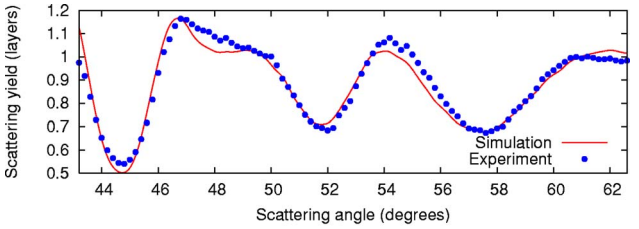

FIG. 6. (Color online) The angle-dependent RE scattering yield from Si(111)1×1-Tm for the $[\bar{1}00]$ incidence geometry shown along with the simulation for the optimum model.

data from both the $[\bar{1}00]$ and $[1\bar{1}\bar{1}]$ incidence scattering geometries. While the vibrational amplitudes of surface atoms were not formally optimized, they were set to values similar to those found to be appropriate in MEIS studies of another 2D silicide[14] which resulted in a reasonable level of agreement between simulation and experiment in terms of dip depths. The final vibrational amplitudes selected were found to result in a sufficiently good fit that the correct operation of the *R*-factor was not impaired. The results of the structural analysis are shown in Table I.

Analysis of the experimental data obtained from the 2D RE silicides of Dy, Ho, and Er proceeded according to the methodology described above and the resulting values are shown in Table I together with the data from the recent Si(111)1×1-Y study.[14]

B. Trends in the 2D RE silicides

The data in Table I are entered in order (from top to bottom) of decreasing RE-Si bond length in the bulk silicide compound and it can be seen from the values relating to the lanthanides (i.e., all RE elements except Y) that this is directly related to the decrease in atomic size of the RE atom as *Z* increases across the period, corresponding to the well-known lanthanide contraction.[23] A generally similar trend can be seen in the values of the RE-Si2 bond length in the 2D RE silicides as determined by MEIS.

The information relating to the bulk silicides[4] clearly indicates that increases in the size of the RE atom result in corresponding increases in the *a*-axis lattice constant and hence the level of lattice mismatch with the Si(111) surface. In the case of the 2D silicides, the *a*-axis parameter of the overlayer is constrained by the substrate periodicity and one might reasonably anticipate that the overlayer is subject to lateral stress as a result. In this regard, it is instructive to examine variations in layer spacing in the direction (which we define as *z*) perpendicular to the surface plane since this axis lies perpendicular to the direction of the applied stress.

The values of the bulk RE-Si layer spacing and the RE-Si2 layer spacing in the 2D silicides are tabulated in Table I and plotted against bulk RE-Si bond length (which represents a measure of the size of the RE atom) in Fig. 7. This plot illustrates a trend in both the RE-Si layer spacing of the bulk RE silicides (as one would expect) and a similar trend in the RE-Si2 layer spacings of the 2D silicides as determined by MEIS. Closer inspection of the plot reveals that while the two traces show the same trend, the variation in the RE-Si layer spacing in the 2D silicides is much stronger than in the case of the bulk silicides.

One possible explanation for the unexpectedly strong variation in the RE-Si2 layer spacing in the 2D RE silicides is that it is related to the presence of strain in the overlayer

TABLE I. Structural parameters obtained from MEIS studies of the 2D RE silicides formed by a range of RE metals on Si(111). Data for the bulk RE silicides is shown for comparison (Ref. 4).

	2D silicide			Bulk silicide[a]		
	Layer spacing/Å		Bond length/Å	Layer spacing/Å	Bond length[b]/Å	Lattice mismatch
Element	RE-Si2	RE-Si1	RE-Si2	RE-Si	RE-Si	
Gd	1.94±0.02	2.80±0.02	2.95±0.01	2.086	3.060	0.96%
Y[c]	1.89±0.02	2.69±0.03	2.91±0.01	2.072	3.035	0.05%
Dy[d]	1.87±0.02	2.68±0.03	2.90±0.01	2.061	3.023	−0.24%
Ho[d]	1.86±0.02	2.69±0.02	2.89±0.01	2.054	3.012	−0.63%
Er[d]	1.85±0.02	2.67±0.02	2.89±0.01	2.044	2.998	−1.10%
Tm	1.82±0.01	2.66±0.01	2.87±0.01	2.044	2.979	−1.88%

[a]These values have been calculated from the *a*- and *c*-axis lattice constants from Ref. 4.
[b]Calculated using the assumption of a perfect AlB_2 structure.
[c]Values for Si(111)1×1-Y are taken from Ref. 14.
[d]The experimental data on which these analyses are based has previously been reported in Refs. 12 and 13.

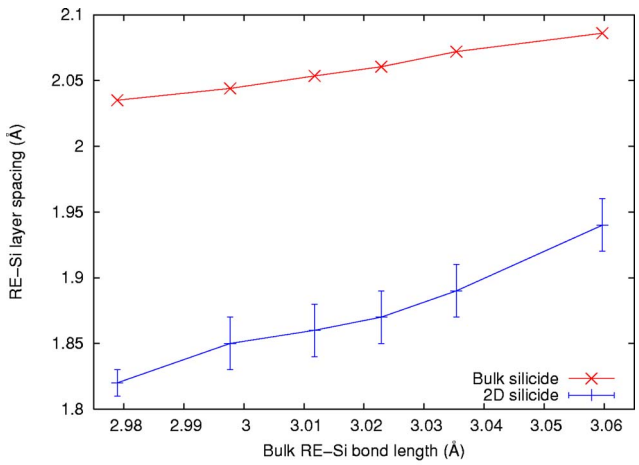

FIG. 7. (Color online) Variations in the RE-Si layer spacing in the bulk RE silicides and the RE-Si2 layer spacing in the 2D silicides plotted against bulk RE-Si bond length (a measure of the size of the RE atom). Lines are drawn between the points to guide the eye. The data relating to the bulk silicides is from Ref. 4.

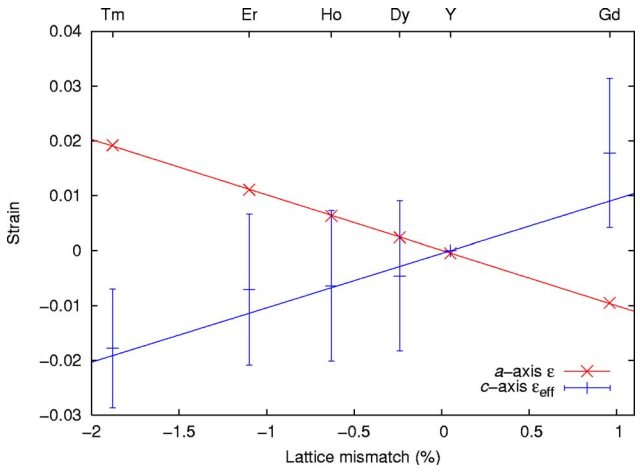

FIG. 8. (Color online) Variations in the effective *c*-axis strain ε_{eff} in the 2D RE silicides plotted as a function of the lattice mismatch between the bulk silicide and the Si(111) surface. The *a*-axis strain (which is defined by the lattice mismatch) is plotted as an aid to the illustration. Each line plotted is a straight-line fit to the associated data points.

which arises as a result of the lattice mismatch with the substrate. In a bulk material the Poisson ratio gives the relationship between an applied tensile strain and the resulting strain in the direction normal to the applied stress—in a perfectly elastic material this acts so as to maintain a constant volume. A similar effect may be envisaged in the case of the 2D RE silicides, namely the compensation of lattice mismatch by changes in the RE-Si layer spacing so as to resist changes in the density of the overlayer. Ideally, one would wish to study the structure of the 2D silicides grown on Si(111) in comparison with those grown on a strained Si(111) surface that had the same *a*-axis lattice constant as the bulk RE silicide in question. While such data is not available, the existence of a series of chemically very similar RE elements with bulk silicides having a range of lattice matches to Si(111) means it is still worthwhile examining the MEIS data for the 2D RE silicides to see if there is evidence for a conservation of density effect.

An alternative way of expressing the trend in the RE-Si layer spacing in the 2D RE silicides is to normalize out the effect of changes in the RE atom size by examining the ratio of the layer spacing in the 2D silicide to that in the bulk compound. If z_{2D} and z_{bulk} are the layer spacings in the 2D silicide and bulk silicide, respectively, then the resulting layer spacing ratio is written as z_{2D}/z_{bulk} and a similar ratio d_{2D}/d_{bulk} can be formed for the corresponding bond lengths. When the ratio d_{2D}/d_{bulk} is calculated for the silicides of the RE metals listed in Table I the resulting value is to a very good approximation a constant, indicating that this ratio is independent of the size of the RE atom. In contrast, the ratio z_{2D}/z_{bulk} shows a significant variation from one RE element to another, a variation which is consistent with the trend illustrated in Fig. 7 and suggests that lattice mismatch contributes to the trend in the RE-Si2 layer spacing in the 2D silicides.

Having established that the variation in z_{2D}/z_{bulk} is likely to be due to a lattice mismatch effect, it is important to identify other contributions to z_{2D}/z_{bulk} which may occur. It is known that the nature of the RE-Si bond in the 2D silicides is subtly different to that in the bulk silicides (despite the close similarity in bond length) since in the former case the relevant Si atoms are part of a buckled Si bilayer (similar to that found in bulk Si) whereas in the latter the Si atoms are contained within a coplanar, graphite-like layer of Si atoms that includes vacancies. Furthermore, it is well known that layer spacings at surfaces are often slightly modified due to relaxation of the surface which is favored by the reduced coordination of surface atoms. Since the effect of the RE atom size has already been normalized out of the ratio z_{2D}/z_{bulk} it is convenient to exploit the fact that it is known that the bulk silicide of yttrium has a near-perfect lattice match (only 0.05% mismatch) to the Si(111) surface. Examining changes in the 2D/bulk RE-Si layer spacing ratio relative to the value calculated for yttrium leads to the expression

$$\varepsilon_{\text{eff}} = \frac{z_{2D}}{z_{\text{bulk}}} - \frac{z_{2D}^{\text{yttrium}}}{z_{\text{bulk}}^{\text{yttrium}}}$$

which is a quantity that is dimensionless, like strain, and also takes a form which is analogous to $\Delta z/z$. It is labelled as an effective strain ε_{eff} to reflect the fact that this calculation is an approximation and one would wish to employ data from a strained Si substrate in an exact calculation, as explained above.

The values of the effective *c*-axis strain ε_{eff} calculated from the MEIS determinations of the 2D RE silicide structure and the bulk silicide data of Ref. 4 are plotted for a range of RE metals in Fig. 8 as a function of lattice mismatch of the bulk silicide with Si(111). To aid the illustration, the corresponding *a*-axis strain is also plotted, although it should be noted these values are defined by the abscissa of the graph so the information that this trace conveys is formally redundant.

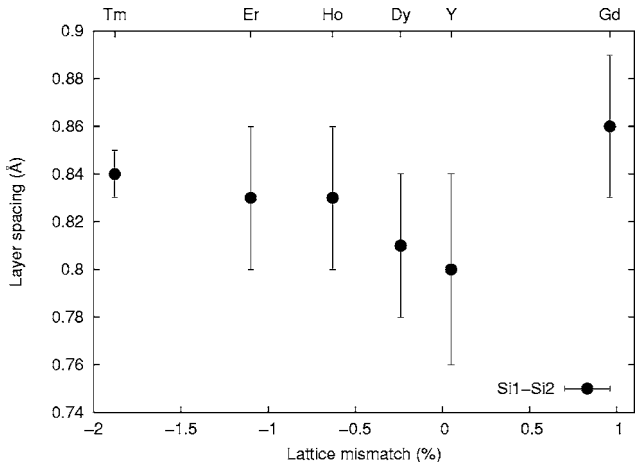

FIG. 9. Variations in the surface bilayer rumple (Si1-Si2 layer spacing) in the 2D RE silicides plotted as a function of the lattice mismatch between the bulk silicide and the Si(111) surface.

The graph in Fig. 8 shows an interesting correlation between the *a*-axis strain that arises from the overlayer being laterally expanded or compressed to fit the substrate, and the resulting effective *c*-axis strain of the silicide. By definition, the effective strain in the 2D silicide of yttrium is zero. The 2D silicide of a large RE element such as Gd (lattice mismatch 0.96%) results in an overlayer which is compressed to fit the substrate and it can be seen that there is a positive ε_{eff} corresponding to an increase in the *c*-axis dimension that acts to compensate the lateral strain. In contrast, the 2D silicide of a small RE element such as Tm (lattice mismatch −1.88%) is expanded to fit the Si(111) surface which gives rise to a negative ε_{eff} corresponding to a decrease in the *c*-axis length.

Finally, the other piece of information contained in the RE scattering yield from the 2D RE silicides, namely the position of atom Si1, was examined. Since Si1 atoms are directly bonded to Si2 atoms, this data is conveniently expressed as the Si1-Si2 layer spacing (alternatively referred to as the bilayer rumple). The relevant data from Table I are plotted in Fig. 9. It can be seen that the 2D RE silicide that has the smallest surface bilayer rumple is that formed by yttrium. The value of 0.80±0.04 Å in this case is closest to the value of 0.78 Å found for a Si bilayer in bulk Si. In the case of the other RE silicides which have a poorer lattice match to Si(111), the trend indicated by Fig. 9 is an increase in the Si1-Si2 layer spacing along with lattice mismatch. This effect appears to be independent of the sign of the lattice mismatch, i.e., both lateral compression and expansion of the silicide layer results in an increase in the surface bilayer rumple in comparison to the yttrium (near-perfect lattice match) value. Such behavior suggests that the presence of lateral strain in the 2D silicide results in a weakening of the Si1-Si2 bond.

IV. SUMMARY AND CONCLUSIONS

The surface structures of the 2D RE silicides Si(111)1 × 1-Gd and Si(111)1 × 1-Tm have been determined using MEIS, and the results of MEIS structural studies of the 2D silicides formed by a range of RE elements have been drawn together to identify trends in this system. It has been found that care is needed in selecting nonstructural parameters in order that the *R*-factor chooses the model which is structurally the best fit and that by taking account of these nonstructural parameters one is able to refine MEIS structural analyses. This is necessary to achieve the level of accuracy required in MEIS analyses that seek to identify subtle variations in structural parameters, such as is the case in the search for trends in the 2D RE silicides.

These data have shown that the RE-Si2 bond lengths in the 2D RE silicides follow the same trend as the RE-Si bond lengths in the bulk silicides, indicating that the bond length changes in the 2D silicides are related to the size of the RE atom. A study of the RE-Si2 layer spacings in the 2D silicides has shown that these values follow a similar trend based on the size of the RE atom, however the variation of this parameter in the 2D silicides is stronger than that of the analogous parameter in the bulk silicides. This has been interpreted in terms of a conservation of density effect that arises due to the differing degrees of lattice match of the bulk silicides of a range of RE metals with the Si(111) surface. It was found that the lateral strain that results in the overlayer being expanded or compressed to fit the substrate is compensated by changes in the RE-Si2 layer spacing.

The surface bilayer rumple (Si1-Si2 layer spacing) in the 2D RE silicides has been compared for a number of RE elements and a pattern has also been found in this parameter. The spacing is smallest at 0.80±0.04 Å in the case of the 2D silicide formed by yttrium (the bulk silicide of which has an almost ideal lattice match with the Si substrate). This is slightly expanded in comparison to the 0.78 Å of a bulklike Si bilayer, however the two values are in agreement within error. The other 2D RE silicides all feature slightly expanded surface bilayers, where the degree of expansion depends on the magnitude of the lattice mismatch of the bulk silicide. This suggests that the presence of lateral strain in the 2D silicides leads to a weakening of the Si1-Si2 bond.

ACKNOWLEDGMENTS

The authors are grateful for the assistance of Dr. K. Connell and the technical support provided by M. Pendleton at Daresbury Laboratory. We should like to thank Dr. P. D. Quinn for supplying the XVegas code and the FOM Institute, Amsterdam for donating the original Vegas code on which the current code is based. We acknowledge financial support from the Engineering and Physical Sciences Research Council (EPSRC) for this research and also EPSRC support of the UK National MEIS Facility at Daresbury Laboratory.

*Electronic address: spt1@york.ac.uk

[1] F. P. Netzer, J. Phys.: Condens. Matter **7**, 991 (1995).
[2] H. Norde, J. de Sousa Pires, F. d'Heurle, F. Pesavento, S. Petersson, and P. A. Tove, Appl. Phys. Lett. **38**, 865 (1981).
[3] K. N. Tu, R. D. Thompson, and B. Y. Tsaur, Appl. Phys. Lett. **38**, 626 (1981).
[4] J. Knapp and S. Picraux, Appl. Phys. Lett. **48**, 466 (1986).
[5] P. Paki, U. Kafader, P. Wetzel, C. Pirri, J. C. Peruchetti, D. Bolmont, and G. Gewinner, Phys. Rev. B **45**, 8490 (1992).
[6] P. Wetzel, C. Pirri, P. Paki, D. Bolmont, and G. Gewinner, Phys. Rev. B **47**, 3677 (1993).
[7] M. H. Tuilier, P. Wetzel, C. Pirri, D. Bolmont, and G. Gewinner, Phys. Rev. B **50**, 2333 (1994).
[8] M. Lohmeier, W. J. Huisman, G. ter Horst, P. M. Zagwijn, E. Vlieg, C. L. Nicklin, and T. S. Turner, Phys. Rev. B **54**, 2004 (1996).
[9] H. Kitayama, S. P. Tear, D. J. Spence, and T. Urano, Surf. Sci. **482–485**, 1481 (2000).
[10] C. Bonet, D. J. Spence, and S. P. Tear, Surf. Sci. **504**, 183 (2002).
[11] C. Rogero, C. Polop, L. Magaud, J. L. Sacedón, P. L. de Andrés, and J. A. Martín-Gago, Phys. Rev. B **66**, 235421 (2002).
[12] D. J. Spence, S. P. Tear, T. C. Q. Noakes, and P. Bailey, Phys. Rev. B **61**, 5707 (2000).
[13] D. J. Spence, S. P. Tear, T. C. Q. Noakes, and P. Bailey, Surf. Sci. **512**, 61 (2002).
[14] T. J. Wood, C. Bonet, T. C. Q. Noakes, P. Bailey, and S. P. Tear, Surf. Sci. (to be published).
[15] C. Preinesburger, S. Vandré, T. Kalaka, and M. Dähne-Prietsch, J. Phys. D **31**, L43 (1998).
[16] J. Nogami, B. Z. Liu, M. V. Katkov, C. Ohbuchi, and N. O. Birge, Phys. Rev. B **63**, 233305 (2001).
[17] P. Bailey, T. C. Q. Noakes, and D. P. Woodruff, Surf. Sci. **426**, 358 (1999).
[18] R. M. Tromp and J. F. van der Veen, Surf. Sci. **133**, 159 (1983).
[19] J. F. Frenken, J. F. van der Veen, and R. M. Tromp, Nucl. Instrum. Methods Phys. Res. B **17**, 334 (1986).
[20] The XVegas software was provided by Dr. P. D. Quinn., URL http://physweb.spec.warwick.ac.uk/~sppq/
[21] T. C. Q. Noakes, P. Bailey, and D. P. Woodruff, Nucl. Instrum. Methods Phys. Res. B **136–138**, 1125 (1998).
[22] I. M. Scott, Ph.D. thesis, Department of Physics, University of York, U.K., 2004.
[23] K. N. R. Taylor and M. I. Darby, *Physics of Rare Earth Solids* (Chapman and Hall, London, 1972).
[24] Except for the case of Er, where a slightly higher value was found necessary. This could be a result of the data for this surface being collected some considerable time before the other data, and thus the exact positioning of the analyzer may have changed at some point.